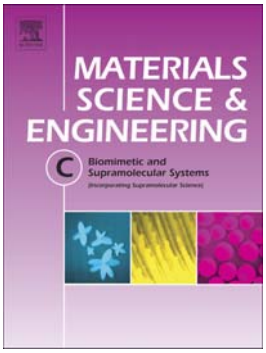

In-situ synthesis of magnetic iron-oxide nanoparticle-nanofibre composites using electrospinning

Luke Burke, Chris J. Mortimer, Daniel J. Curtis, Aled R. Lewis, Rhodri Williams, Karl Hawkins, Thierry G.G. Maffeis, Chris J. Wright

PII: S0928-4931(16)31186-9
DOI: doi: 10.1016/j.msec.2016.09.014
Reference: MSC 6896

To appear in: *Materials Science & Engineering C*

Received date: 28 April 2016
Revised date: 15 August 2016
Accepted date: 6 September 2016

Please cite this article as: Luke Burke, Chris J. Mortimer, Daniel J. Curtis, Aled R. Lewis, Rhodri Williams, Karl Hawkins, Thierry G.G. Maffeis, Chris J. Wright, In-situ synthesis of magnetic iron-oxide nanoparticle-nanofibre composites using electrospinning, *Materials Science & Engineering C* (2016), doi: 10.1016/j.msec.2016.09.014

In-situ synthesis of magnetic iron-oxide nanoparticle-nanofibre composites using electrospinning

*Luke Burke[12], Chris J. Mortimer[12], Daniel J. Curtis[2], Aled R. Lewis[2], Rhodri Williams[2], Karl Hawkins[3], Thierry G. G. Maffeis[2], Chris J. Wright[123]**

1. Biomaterials, Biofouling and Biofilms Engineering Laboratory (B^3EL), Systems and Process Engineering Centre, College of Engineering, Swansea University, Fabian Way, Swansea, SA1 8EN, UK

2. Systems and Process Engineering Centre, College of Engineering, Swansea University, Fabian Way, Swansea, SA1 8EN, UK

3. Centre for NanoHealth (CNH), Swansea University, Singleton Park, Swansea, SA2 8PP, UK

Email: c.wright@swansea.ac.uk

Keywords: Magnetic nanoparticles; magnetite; Electrospinning; Scale-up; Nanoparticle synthesis; nanofibres;

Abstract

We demonstrate a facile, one-step process to form polymer scaffolds composed of magnetic iron oxide nanoparticles (MNPs) contained within electrospun nano- and micro-fibres of two biocompatible polymers, Poly(ethylene oxide) (PEO) and Poly(vinyl pyrrolidone) (PVP). This was achieved with both needle and free-surface electrospinning systems demonstrating the scalability of the composite fibre manufacture; a 228 fold increase in fibre fabrication was observed for the free-surface system. In all cases the nanoparticle-nanofibre composite

scaffolds displayed morphological properties as good as or better than those previously described and fabricated using complex multi-stage techniques. Fibres produced had an average diameter (Needle-spun: 125 ± 18 nm (PEO) and 1.58 ± 0.28μm (PVP); Free-surface electrospun: 155 ± 31 nm (PEO)) similar to that reported previously, were smooth with no bead defects. Nanoparticle-nanofibre composites were characterised using scanning electron microscopy (SEM), energy dispersive x-ray spectroscopy (EDX), dynamic light scattering (DLS) (Nanoparticle average diameter ranging from 8 ± 3nm to 27 ± 5nm), XRD (Phase of iron oxide nanoparticles identified as magnetite) and nuclear magnetic resonance relaxation measurements (NMR) (T1/T2: 32.44 for PEO fibres containing MNPs) were used to verify the magnetic behaviour of MNPs. This study represents a significant step forward for production rates of magnetic nanoparticle-nanofibre composite scaffolds by the electrospinning technique.

1. Introduction

Nanoparticle-nanofibre composites have been subject to a vast amount of research due to their functionality and unique chemical and physical properties[1,2]. Nanofibres (NF) are widely used for a number of different industrial and medical applications and their use has been extended by functionalizing NFs with metal nanoparticles (NP) in areas such as regenerative medicine, sensing, catalysis and microelectronics [3–7]. In any application of NPs, the primary concern is the formation of the desired NPs in the correct size and material composition. There are a number of different fabrication techniques currently used for NP-NF composites, with most involving multiple step procedures. The most commonly used method involves using a suitable method to synthesize nanoparticles, including precipitation and co-precipitation, chemical vapour condensation, reverse micelle mechanism, thermal decomposition, reduction and liquid phase reduction [8] , and subsequently extracting the

nanoparticles and then combining them with a polymer solution to be electrospun [9,10]. Another technique involves adding a metal salt (precursor) to a polymer solution and electrospinning[11]. The fibres can then be treated post fabrication by subjection to thermal, chemical or radiolytic treatment (or combinations thereof) to reduce the metal ions to NPs. More recently, research has focused on developing techniques involving a reduced number of steps. Saquing *et al.* presented a one-step synthesis technique to incorporate silver NPs into Poly(ethylene oxide) (PEO) NFs where silver nitrate ($AgNO_3$) was reduced using PEO as the reducing agent [12].

Magnetic scaffolds have gained attention in a range of fields, however; the relatively slow production rate of such nanostructures has often limited their successful widespread application. The inherent superparamagnetic properties of magnetic NPs (MNPs) are of particular interest, and have been studied for a range of applications including; contrast improvement for magnetic resonance imaging [13], targeted drug delivery [14], gene therapy [15], hyperthermia treatment [16], filtration [17,18], glucose sensing [19], peroxidase mimetic activity [20] and cell separation [21]. Ismail *et al.* have recently shown iron oxide nanoparticles to show antimicrobial properties, inhibiting the growth of both gram-negative and gram-positive bacteria [22]. Cai *et al.* included iron oxide NPs in NFs composed of chitosan and gelatin to improve both mechanical and antibacterial properties [7]. In another recent important publication for the application of MNPs to regenerative medicine, Meng *et al.* reported that the presence of a nanofibrous material containing MNPs inserted within a bone fracture site in a rabbit model increased osteocalcin expression by osteoblasts and improved healing rates over 100 days [23]. In their work, iron particles were pre-synthesised using a modified emulsion technique and then added to a Poly(DL-lactide)/Dimethylacetamide solution along with hydroxyapatite nanoparticles before electrospinning. The authors did not fully discuss the specific electrospinning apparatus or the fabrication methodology other than

that the implant was prepared by addition of pre-synthesised MNPs to an electrospinning system and the resulting nanofibrous mat was folded to produce a 0.5cm^2 construct for bone repair. If it is assumed that the common single-needle electrospinning system was employed this would be an extremely time consuming, multi-stage process. In order for advances in the application of MNPs and functional polymer scaffolds to be translated into commercial viability and widespread testing the fabrication process must be simplified and scaled.

For many biological and medical applications, it is advantageous to include MNPs within a biocompatible scaffold for delivery and retention at a targeted site. Fabrication of these materials is generally two-stage process, with the NPs synthesized separately and then added to a scaffold material. This process presents familiar challenges such as particle agglomeration and uneven distribution throughout the eventual scaffold. In this study, *in-situ* synthesised MNPs within nanofibrous scaffolds were prepared by the co-precipitation technique [24] coupled with electrospinning. This allows for a homogenous distribution of nanoparticles throughout the fibres. Poly (ethylene oxide) (PEO) was chosen as the electrospinning polymer due to its excellent fibre-forming properties, biocompatibility, chemical stability and water solubility, removing the necessity for harsh solvents. In addition, Poly (vinyl pyrrolidone) (PVP) was also used to illustrate the effect of the choice of electrospun polymer on average particle diameter.

Electrospinning has previously been used to immobilise NPs [5,23], however the production rate of conventional electrospinning systems is limited, preventing the technique from being practically applied on a large scale [25]. Examples of free-surface electrospinning processes that directly fabricate fibres containing MNPs are not found in the current literature. The requirement for production of MNP-containing fibres at an industrial scale for *in vivo* or clinical testing makes this research particularly relevant and important for future direction within regenerative medicine and other applications.

To address the issue of low throughput in the presented research, scaffolds were prepared using a one-step technique combining *in-situ* particle synthesis with electrospinning. One where the particle synthesis and polymer solution preparation are carried out in one step, allowing electrospinning to be carried out immediately having only prepared one solutionThe *in-situ* synthesis of magnetic nanoparticles within an electrospinning system allowed for homogenous particle dispersion through sub-micron fibres as well as production scale-up using a commercially available "free-surface" electrospinning system.

2. Experimental Section

2.1. Materials

Poly(ethylene oxide) (PEO) (M_w = 900kDa), Poly(ethylene oxide) (PEO) (Mw = 400kDa), poly(vinyl pyrrolidone) (PVP) (Mw = 55kDa), sodium borohydrate ($NaBH_4$)(≥97% pure), sodium chloride (NaCl) (BioXtra, ≥99.5% pure), ferrous chloride ($FeCl_2$) (96% pure), ferric chloride ($FeCl_3$) (97% pure) and pentaerythritol triacrylate (PETA) (technical grade) were purchased from Sigma Aldrich UK. All water used was millipore-filtered. All reagents were used as received without further purification.

2.2. Solution Preparation

PEO (M_w = 900kDa)/water stock solution was prepared at a concentration of 5%(w/w). PEO (M_w = 400kDa)/water stock solution was prepared at a concentration of 5.5%(w/w). Both PEO stock solutions were supplemented with 10% PETA with respect to polymer weight. PVP/water stock solution was prepared at a concentration of 47%(w/w). Two solutions of ferrous/ferric chloride were mixed at a 2:1 molar ratio to a total iron concentration of 1.3mM and 1.3M. A solution of sodium borohydride (2M) was prepared in deionized water. Both the ferric/ferrous chloride and sodium borohydride solutions were prepared fresh before each experiment.

2.3. Electrospinning via needle-aperture

For electrospinning via a needle-aperture system, each polymer stock solution (25ml, PEO M_w = 900kDa and PVP Mw = 55kDa) was supplemented with sodium borohydride solution (500µL, 2M) and mixed vigorously for 5 minutes to ensure homogenous distribution. Subsequently, the $FeCl_3/FeCl_2$ solution (500µL) was added to the polymer solution. An immediate colour change was observed on addition of the iron solution due to particle formation. The reaction was allowed to proceed for 20 minutes at room temperature under continuous agitation before being loaded into a 5mL syringe. Electrospinning was performed using the PROFECTOR LIFE SCIENCES SPRAYBASE® system with a 16-gauge (I.D. 1.19mm) blunt end stainless steel needle with an aluminium foil collector substrate. Electrospinning parameters were as follows; voltage 15kV (PEO) and 18kV (PVP), feed rate 0.5ml/h and a tip to collector distance of 17cm. The electrospinning process was allowed to proceed for 1 hour before fibres were collected for imaging, at which time a 3x3cm square of the foil collector substrate was removed and imaged directly without sputter coating or other treatments.

2.4. Electrospinning via free-surface technique

To investigate scale-up of the NF production free-surface electrospinning was employed using the EL MARCO NANOSPIDER Lab 200 system. This technique is a relatively recent adaptation to the standard electrospinning approach [26] and is designed to permit the formation of several polymer jets simultaneously in order to scale up fibre production. A schematic diagram showing the free-surface electrospinning set-up employed is presented in **Figure 1.** A five 228-fold increase in fibre production (g/hour) was observed between the needle and free-surface techniques. PEO (40ml, M_w = 400kDa) was added to a 50mL universal container. A different molecular weight PEO was used compared to the needle based process (M_w = 900kDa) this allowed the formation of fibres with similar diameters, while maintaining concentrations within the electrospinning solutions; the solutions were

supplemented with the same amount of precursor for nanoparticle formation. For solutions not containing iron NPs the conductivity of the solution was adjusted by addition of sodium chloride to a value of 3mS/cm. Sodium borohydride (500µL, 2M) was added to the polymer solution and thoroughly mixed for 5 minutes to ensure homogenous distribution. Subsequently, ferric/ferrous chloride solution (500µL) was added drop-wise to the solution. An immediate colour change from clear to black was observed due to particle formation. Conductivity of solutions containing NPs was measured at ~6mS/cm and therefore did not require the addition of sodium chloride. The solution was then directly electrospun onto aluminium foil via the EL MARCO NANOSPIDER Lab 200 system using a 6-wire electrode, a tip-collector voltage of 60kV and a tip-collector distance of 20cm. Under these conditions, the observed tip-collector current varied between 60-100µA, indicating consistent fibre-formation. The electrospinning process was allowed to continue for 15 minutes before a 3x3cm section from the centre of the foil collection substrate was removed for SEM imaging and further characterisation. Scanning electron microscopy was achieved using the Hitachi S4800 at an acceleration voltage of 5kV and emission current of 10µA. To visualize the presence of nanoparticles contained within the fibres Scanning transmission Electron Microscopy (STEM) was used at an acceleration voltage of 30kV and emission current of 20µA.

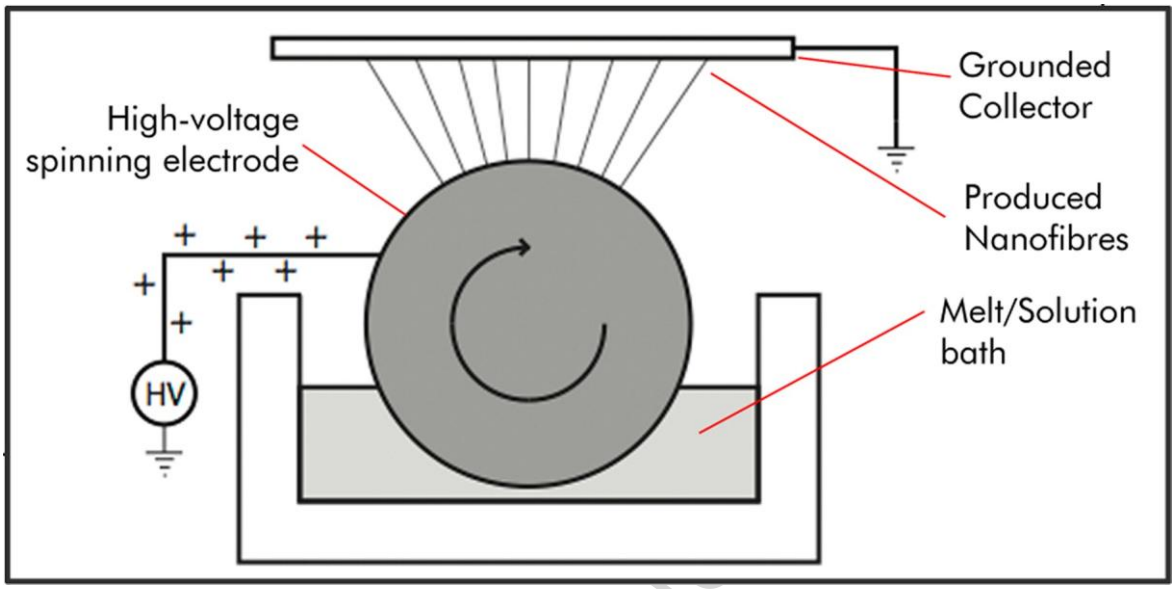

Figure 1. A schematic diagram showing a free-surface electrospinning set-up. A polymer solution/melt is held in a bath and a spinning electrode connected to a high voltage power supply is utilized to form multiple jets. Nanofibres are electrospun upwards and collected on a grounded collector plate.

2.5. X-Ray Diffraction

To determine the state of iron oxide nanoparticles X-Ray Diffraction studies were performed using a Bruker D8 discover x ray diffractomer using a non monochromated Cu K alpha source radiation (wavelength λ=0.1541838nm). For the iron oxide nanoparticle sample the patterns were recorded over 2θ from 10° to 60 ° in 0.0102° increments with the source fixed at θ=2°. For the PEO and sample plate control the samples were scanned using the standard Bragg Brentano 2θ set up from 5° to 54° at 0.04° increments. To increase the signal and help remove alignment errors the PEO nanofibres containing MNPs were dissolved in water, centrifuged to concentrate and dropcast on a silicon wafer (20mmx10mm wide).

2.6. Dynamic Light Scattering

The size of the NPs were analysed using the Malvern Zetasizer Nano. The equipment employs dynamic light scattering (DLS) to size particles present in a liquid medium, by mass and

provide a size distribution and polydispersity index. Initially the PEO and PVP solutions were diluted 10x in filtered, deionized water and examined using the Zetasizer to determine the size of iron oxide NPs formed before the electrospinning process. After electrospinning the formed fibres were dissolved in filtered, deionized water and subsequently examined using the Zetasizer to determine whether particle size had been altered by the electrospinning process.

2.7. Nuclear Magnetic Resonance

Spin-lattice, T1, and spin-spin, T2, proton relaxation time constants of water were measured using an inversion-recovery sequence with a spoiler gradient (which negates the need for phase cycling and hence allows rapid data acquisition [27]) and a Carr-Purcel-Meiboom-Gill (CPMG) spin echo sequence[28], respectively. Measurements were performed on PEO polymer, PVP Polymer, PEO Polymer containing MNPs, PVP Polymer containing MNPs and redissolved PEO electrospun NFs containing MNPs. All samples were diluted 10x in de-ionized water. The iron concentration of the PEO + MNPs sample and the redissolved PEO nanofibres + MNPs sample was kept constant. Measurements were performed on a Bruker Avance III 500 MHz spectrometer fitted with a 10 mm diff30 NMR probe with z-gradient, a 5 mm NMR tube was used in order to reduce the effects of radiation dampening. Three measurements of T1 and T2 were made on each sample.

2.8. Flame Atomic Absorption Spectroscopy

Flame Atomic Absorption Spectroscopy (FAAS) was used to determine the concentration of iron present in the polymer solutions and fibres formed from solution. The FAAS was carried out using a Perkin Elmer PinAAcle 900F spectrophotometer with an iron acetylene lamp using a current of 30mA. The flame emission wavelength was 248.33nm with a slit width of 0.2nm. As the spectrophotometer has an upper limit of 5mg/L the samples needed to be diluted for the analysis. PEO and PVP solutions containing nanoparticles were diluted 115x in deionized water. Electrospun PEO fibres (0.00294g) were dissolved in DI water (6.795ml)

with a ratio 1:2311. PVP fibres (0.01224g) were dissolved in deionized water (3.0174g) a ratio of 1:247.

2.9. Crosslinking of PEO nanofibres containing MNPs formed using free-surface electrospinning

To improve the physical properties of the PEO NFs and make them suitable for applications such as wound dressings and filter membranes the water solubility of the fibres was decreased. UV initiated crosslinking of PEO NFs containing MNPs was achieved by the method previously described by Zhou *et al.* [29] with PETA as both the photo-initiator and crosslinker . UV irradiation was carried out by a Hartmann UV-H 255 hand lamp (Hartmann Feinwerkbau GmbH, Ober-Mörlen, Germany) emitting a light intensity of 100 mW/cm^2 at a wavelength of 320nm to 405nm. Samples were placed under the UV light at a distance of 20cm for 30 minutes. To test the degree of crosslinking samples were vacuum dried and weighed before submersion in deionized water for 24 hours at 25°C. After this time samples were removed and vacuum dried to dry weight to determine the weight loss. SEM imaging was then used to examine the morphology change before after cross linking and immersion studies.

3. Results and Discussion

Scanning Electron Microscopy (SEM) images of electrospun fibres from both needle and free-surface electrospinning systems with and without MNPs are shown in **Figure 2**. To achieve a representative characterization of size distribution 100 fibres were chosen at random from 10 randomly positioned SEM images of each electrospun sample. These fibres were measured using Image J software, and were observed to have an average diameter of 125 ± 18 nm for needle-spun PEO fibres containing MNPs and 155 ± 31 nm for free-surface electrospun PEO fibres containing MNPs. Needle-spun PVP fibres containing MNPs had an

average diameter of 1.58 ± 0.28μm. The morphology of all fibres appeared smooth, with homogeneous diameters and an even dispersion of MNPs within the fabricated nonwoven mat. These results are comparable with those of other research groups, who reported average diameters of both PEO and PVA electrospun NFs containing MNPs as 150-250 nm [9,30]. Figure 2c illustrates the potential for increased iron content within the fibres, with a thousand-fold increase causing only slight beading of the fibres. This wider range of iron concentrations allows the technique to be adapted to a range of applications' requirements.

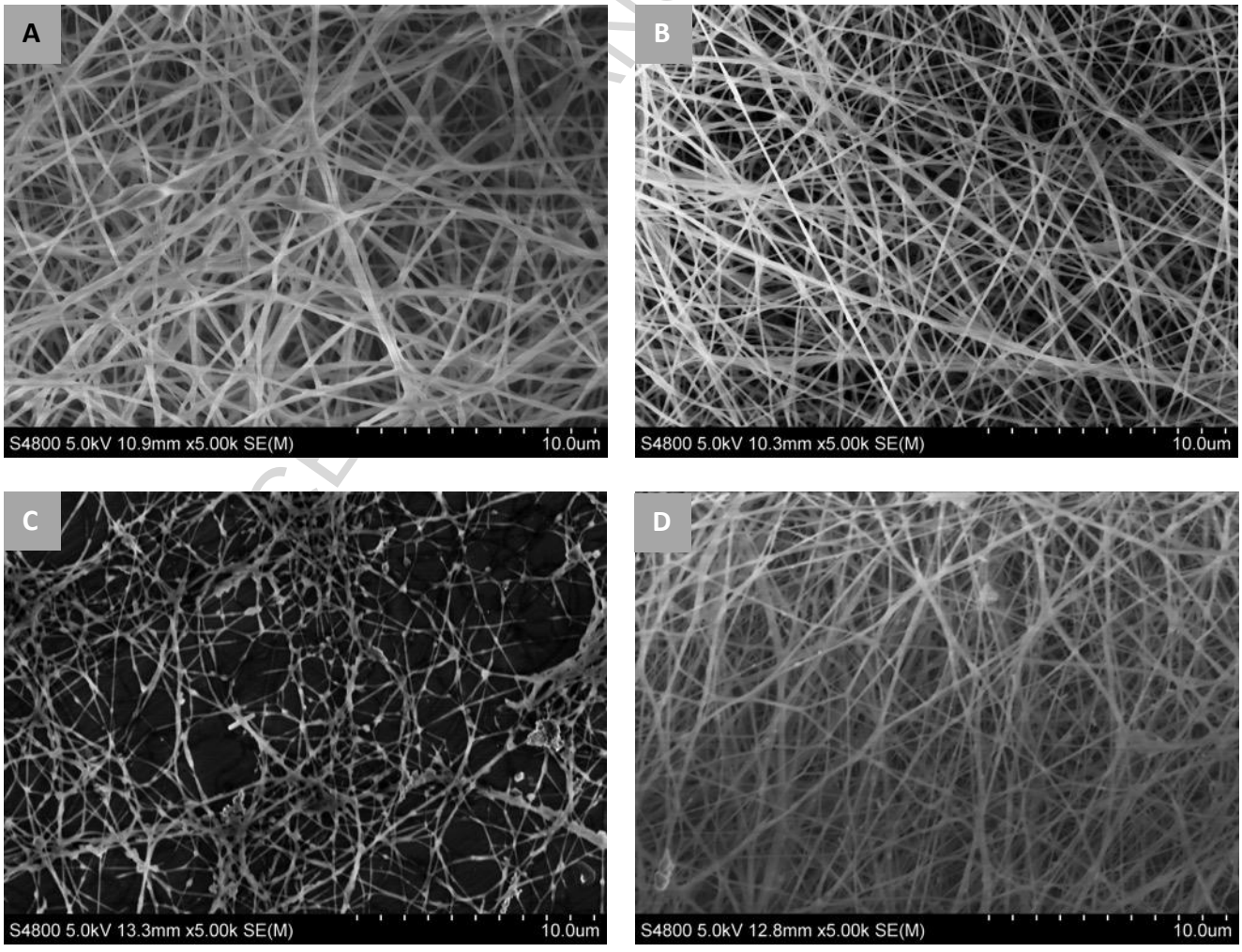

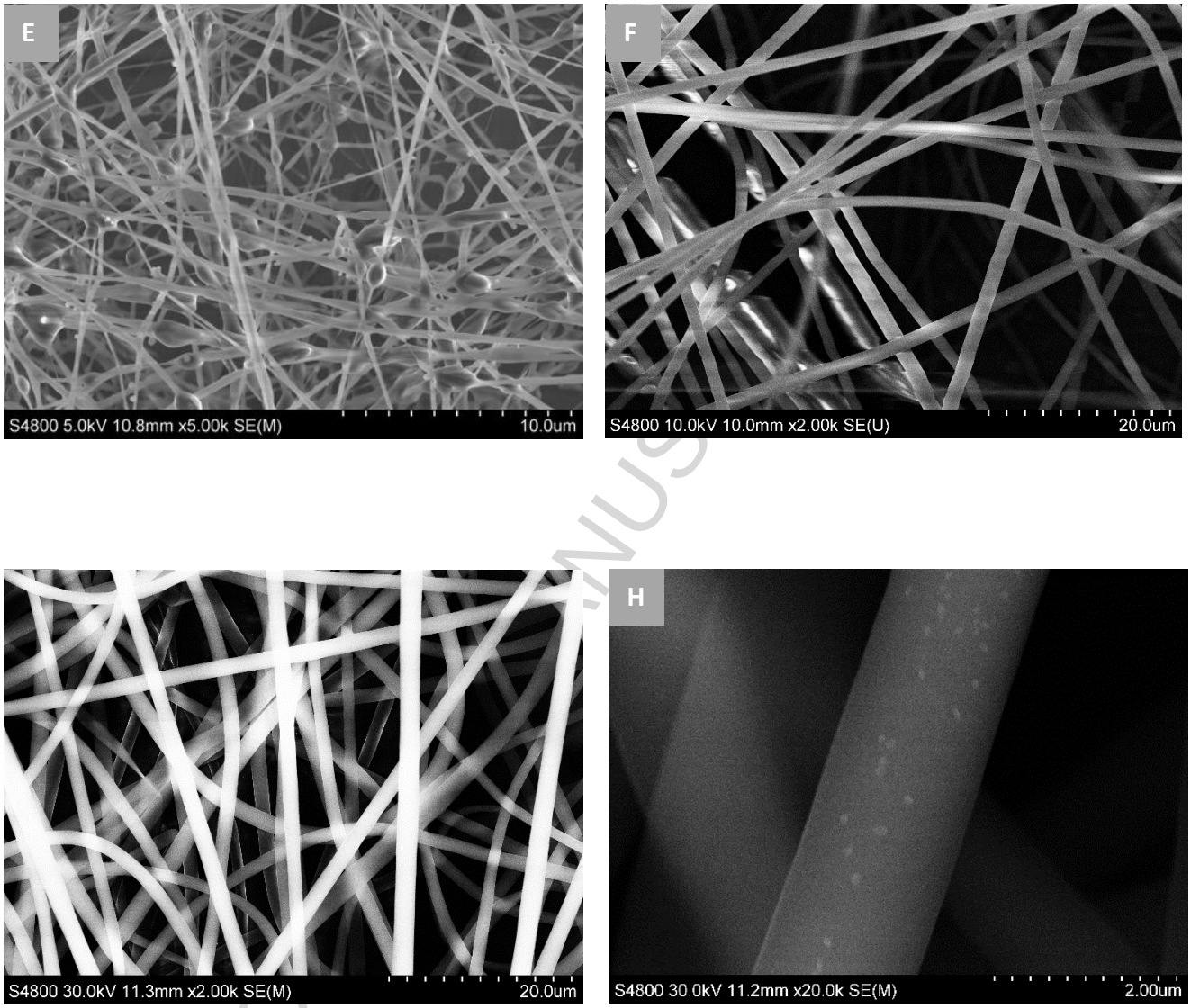

Figure 2. SEM images of electrospun PEO and PVP nanofibres with and without *in-situ* synthesised magnetic iron-oxide nanoparticles (a) PEO nanofibres formed from 5%(w/w) PEO in DI water (b) PEO nanofibres containing MNPs with total iron concentration of 1.3mM (c) PEO nanofibres containing MNPs with total iron concentration of 1.3M (d) PEO nanofibres formed from 5.5%(w/w) PEO in DI water containing 0.01% NaCl electrospun via a free-surface electrospinning system (e) PEO nanofibres containing MNPs with total iron concentration 0f 1.3mM electrospun via the free-surface electrospinning (f) PVP microfibres (g) PVP microfibres containing MNPs with total iron concentration of 1.3mM (h) PVP microfibres with total iron concentration of 1.3mM.

To measure fibre production rates, foil substrates were weighed before and after electrospinning. Under the specified conditions the maximum rate for the needle-spinning system was 0.0219 g/hr, which is consistent with the rate established by other groups [31]. However, when electrospun using a free-surface electrospinning system the production rate was increased to approximately 5 g/hr, a 228-fold increase, with no negative effects on the key quality indicators of fibre size and degree of polymer beading in the fabricated NF mats. This demonstrates the scale-up of the process and the potential for significant manufacturing production rates as the commercial free-surface system (El-Marco Nanospider lab 200) used in the present study has been further scaled to process plant. Size distributions are shown in **Figure 3** and SEM images used for measurements are available in supplementary information.

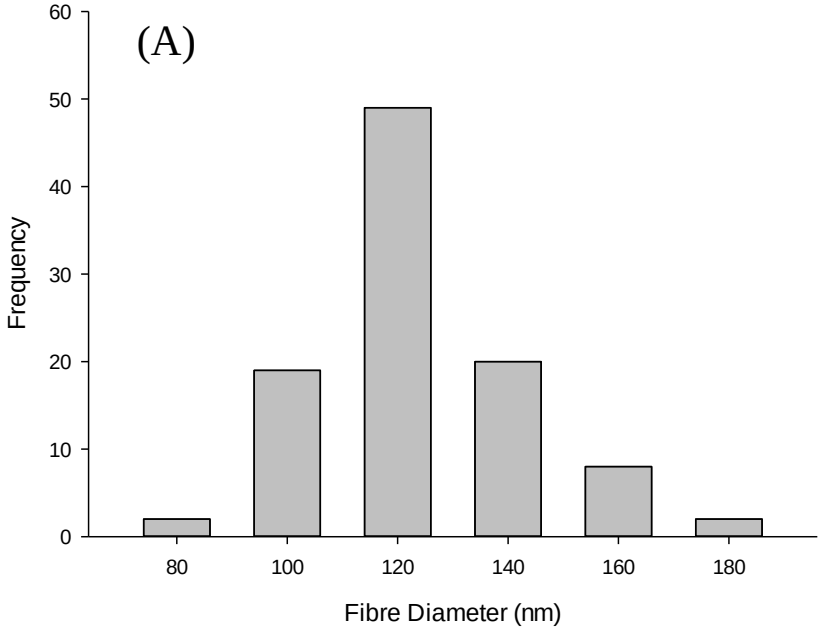

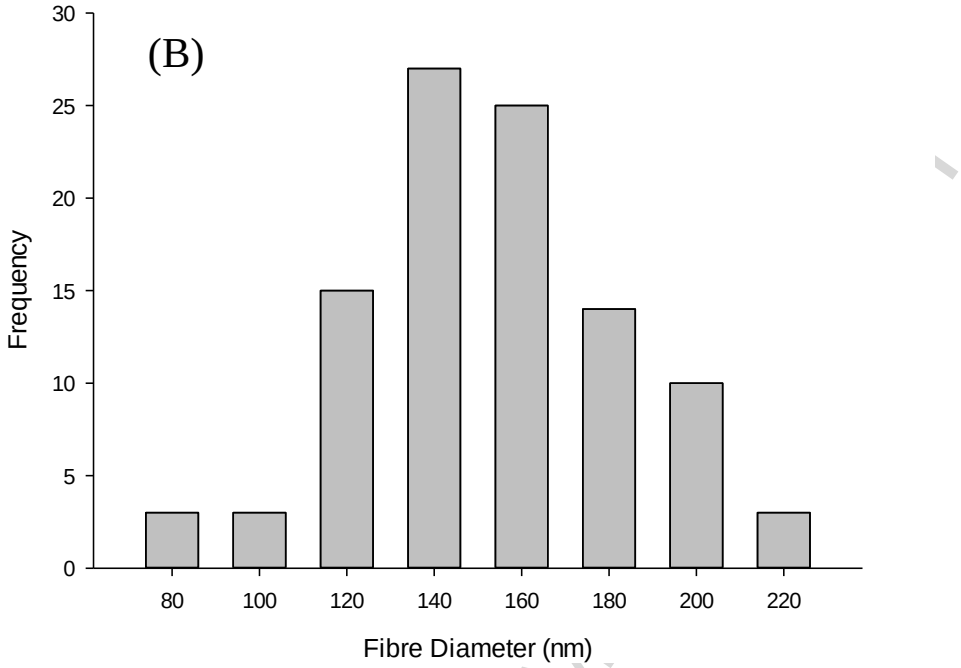

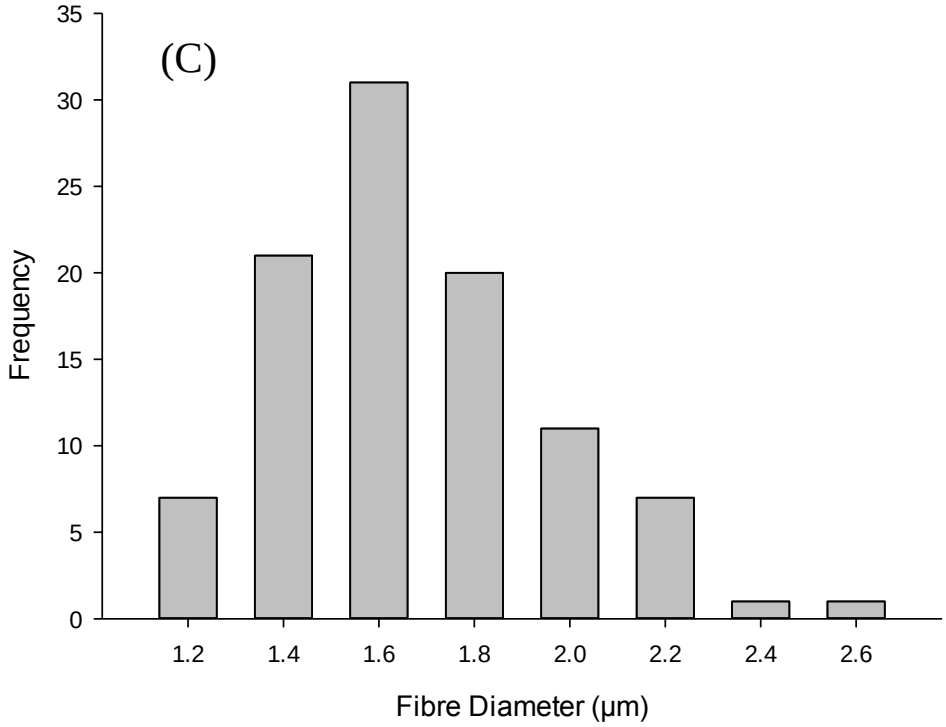

Figure 3. Size distribution data from 100 randomly chosen fibres; (A) Needle spun PEO fibres with MNPs (Average fibre diameter 125.34 ± 18.17 nm) (B) Free-surface

electrospun PEO fibres with MNPs (Average fibre diameter 154.98 ± 30.86 nm) (C) Needle spun PVP fibres with MNPs (Average fibre diameter 1.58 ± 0.28μm).

Figure 4 shows a high magnification Scanning Transmission Electron Microscopy (STEM) image. The STEM images clearly show the presence of NPs within the electrospun fibres.

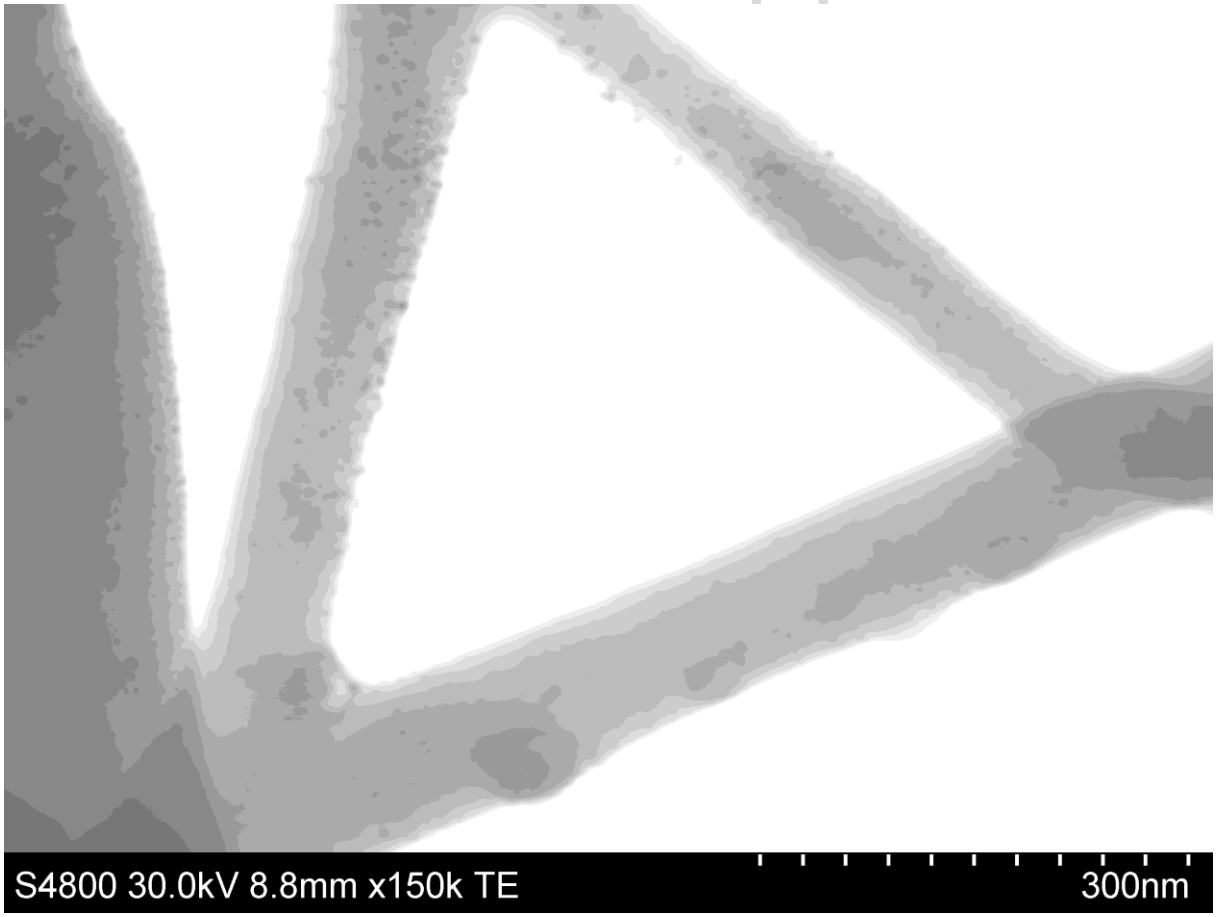

Figure 4. High magnification Scanning Transmission Electron Microscopy image of PEO nanofibre containing MNPs.

Table 1 shows results of Dynamic Light Scattering characterization of the formed MNPs in both the pre-electrospun solutions and the re-dissolved electrospun fibres. Pre-electrospinning, the average particle size was 8 ± 3 nm in PVP and 13 ± 2 nm in PEO. Some aggregation of the particles appears to have occurred during the electrospinning process as the average size

of particles in PVP increased to 10 ± 4 nm and to 27 ± 4 nm. However, this effect is likely exaggerated due to particles aggregating during fibre dissolution, as STEM images of the electrospun fibres clearly show smaller encapsulated particles. Particle sizes were smaller in PVP than PEO, which is most likely explained by the stabilising effects of the polymer. PVP is more generally used [32] as it has a greater stabilising effect than PEO, through adsorption of the polymer chains onto the NP surface lowering their surface energy and preventing further aggregation [33]. Particles formed in the presence of PVP are similar to those described by other research groups, for example H-Y Lee *et al.* [34] synthesised particles of diameter 8 – 10nm in the presence of PVP.

Table 1. Particle size average ± standard deviation (nm) of MNPs via dynamic light scattering.

Polymer	**Pre-electrospinning (nm)**	**Post-electrospinning (nm)**
PEO	13±2	27±5
PVP	8 ± 3	10 ± 4

To verify that the visualised particles contained iron *in-situ* Energy Dispersive X-Ray spectroscopy (EDX) was performed in point-identification mode on particles visualised via STEM. **Figure 5** shows EDX spectra and associated SEM images, in which the particles are clearly identified as containing iron. Both sodium and chlorine are present from the precursors. Copper and silicon are also shown to be present, copper from the clip used to retain the sample and silicon was present on the SEM stub. Due to the particles being formed *in-situ* within the polymer fibres the oxide peak from the polymer masks the ratio of iron to oxygen. Therefore, the iron-oxide NPs could not be discerned as being magnetite, maghemite, hematite or some other non-magnetic iron oxide compound via EDX alone.

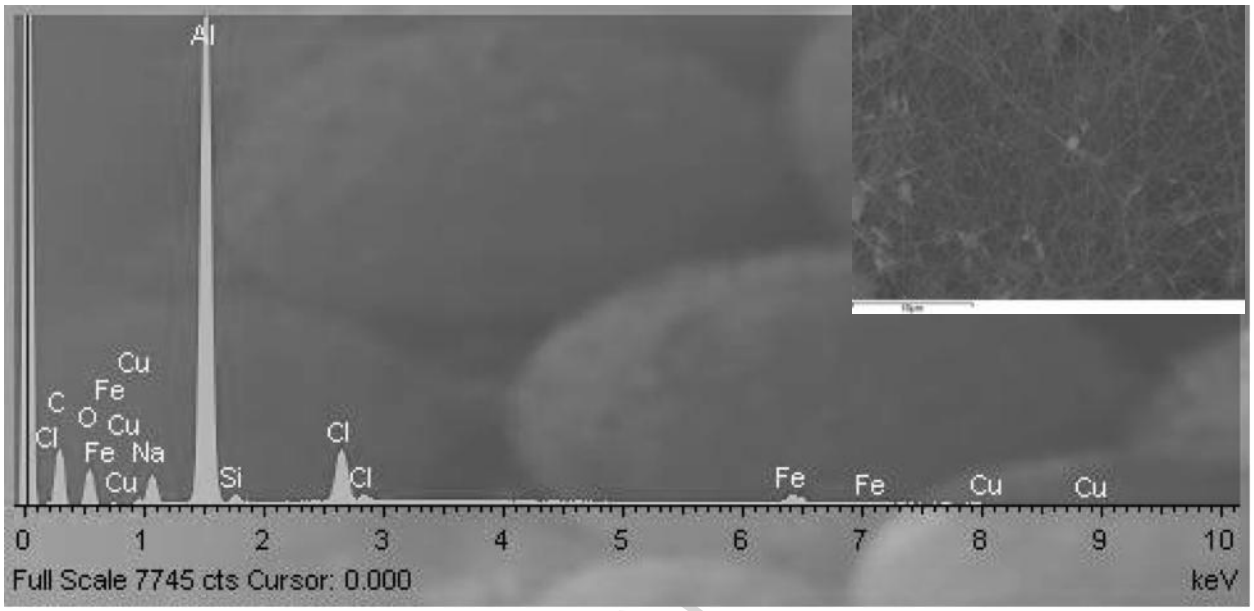

Figure 5. EDX Point-ID Spectra and associated SEM image of MNPs within electrospun PEO nanofibres (inset).

To determine the state of iron oxide nanoparticles present XRD analysis was performed and the resultant scans were compared to that of magnetite (AMCSD 0000945), maghemite (AMCSD 0007898) and hematite (AMCSD 0000143).

Figure 6 shows the XRD patterns for the iron oxide nanoparticles. Upon inspection the presence of the (311), (400), (333), (111), (422) and (220) reflections corresponding to magnetite were found ((311) fitted envelope in supplementary information). The presence of magnetite peaks and the lack of peaks corresponding to maghemite and hematite suggests that the particles formed in-situ are magnetite in phase. (Control patterns can be found in the supplementary information)

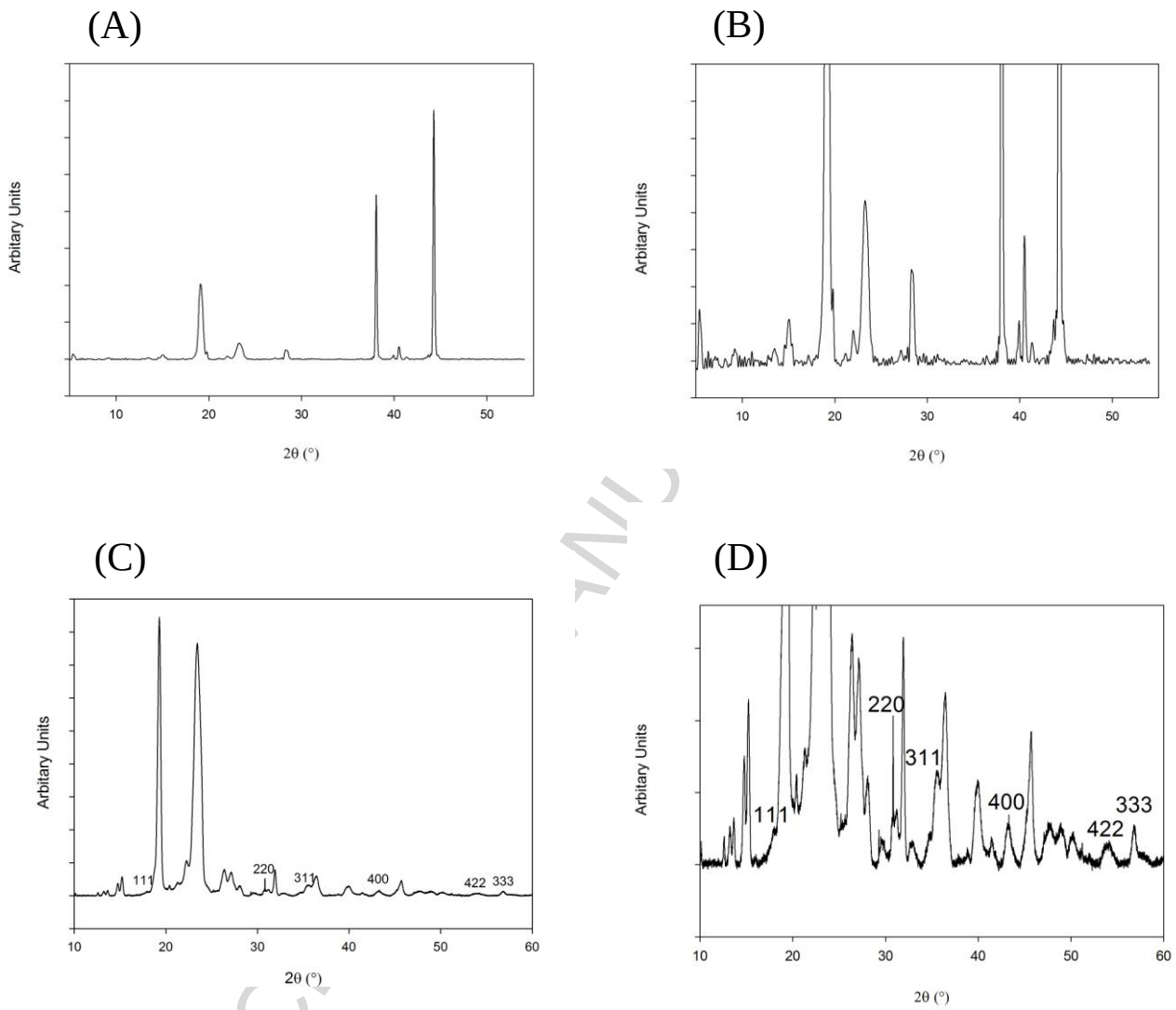

Figure 6. XRD patterns for (A) PEO nanofibres containing NaCl, (B) PEO nanofibres containing NaCl (magnified), (C) PEO nanofibres containing MNPs and (D) PEO nanofibres containing MNPs (magnified).

Nuclear Magnetic Resonance (NMR) relaxation measurements were used to verify the magnetic behaviour of the iron nanoparticles formed within electrospun fibres. This was achieved by measuring spin-lattice (T_1) and spin-spin (T_2) relaxation times of water protons in pre-electrospun solutions as well as those extracted by dissolution of NFs. A shortening of both T_1 and T_2 relaxation time constants was observed (**Table 2**) in the presence of iron oxide

NPs, both in pre-electrospun solutions as well as re-dissolved electrospun fibres. This reduced relaxation time is consistent with the presence of an efficient relaxation channel provided by the magnetic moment of the iron oxide NPs [35].

Table 2. Nuclear Magnetic Resonance Spectroscopy results of *in-situ* synthesised MNPs.

Sample	T_1 (ms)	T_2 (ms)	T_1/T_2
PEO	3114 ± 24	2387 ± 5	1.46
PEO + MNPs	2981 ± 2	92 ± 4	32.44
Redissolved electrospun PEO nanofibres	2955± 31	283 ± 54	10.69
PVP	3016 ± 3	1943 ± 70	1.55
PVP + MNPs	2717 ± 7	974 ± 2	2.79

Flame Atomic Absorption Spectroscopy (FAAS) was employed to measure the total iron concentration of the pre-electrospun solutions as well as dissolved fibres. This was to ensure that no iron content was lost due to particles settling during the electrospinning process, or being poorly transferred in the electrospun jet during free-surface electrospinning. Due to the PEO solution being 5% (weight-weight) in water, the post-electrospinning iron concentration was expected to increase twenty-fold, as a result of water loss during the electrospinning process. Similarly, the post-electrospinning iron concentration was expected to double for the PVP fibres due to the solution being ~50% (weight-weight) in water. **Table 3** shows FAAS results obtained from these experiments, illustrating an approximately twenty-fold increase for PEO and two-fold increase for PVP as expected and, therefore, a consistent iron

concentration throughout electrospinning fibre formation with no losses due to particle settling or poor transfer.

Table 3. Flame Atomic Absorption Spectroscopy of iron content pre- and post-electrospinning

Sample	Iron Concentration (mg/g)
PEO Pre-electrospinning	0.124
PVP Pre-electrospinning	0.115
PEO Post-electrospinning	2.44
PVP Post-electrospinning	0.261

PEO fibres are water-soluble and so require a cross-linking step prior to application within an aqueous environment. UV initiated crosslinking of PEO NFs containing MNPs was performed with pentaerythritol triacrylate (PETA) as both the photo-initiator and crosslinker as previously described by Zhou *et al.* [29]. UV irradiation results in PETA in an excited triplet state allowing hydrogen absorption on the PEO molecule. This results in the formation of PEO and PETA radicals, which undergo polymerization and radical coupling to form a PEO-PETA molecule, which is water insoluble. This was confirmed by solubility tests where the samples did not lose any significant weight after being submersed in DI water for 24 hours at 25°C. The presence of the cross linker did not change NF or NP morphologies or compromise the increase in volume throughput for the free-surface electrospinning system. SEM images of crosslinked PEO nanofibres containing MNPs electrospun using a free-surface electrospinning set up, pre and post immersion are presented in Figure 7.

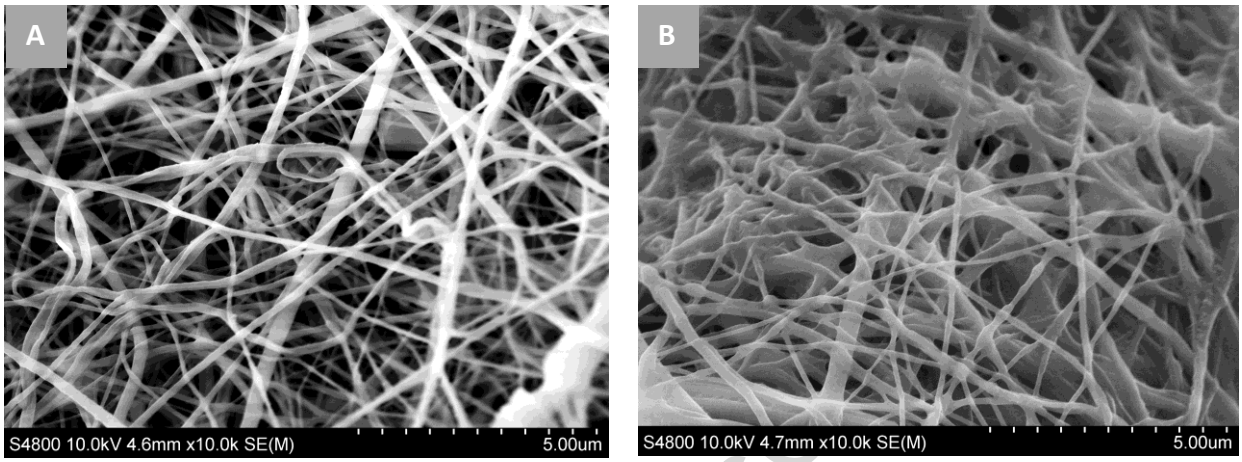

Figure 7. SEM images of crosslinked PEO nanofibres containing MNPs (a) Before submersion in DI water and (b) After submersion in DI water.

4. Conclusion

We have successfully developed a novel high throughput method for *in-situ* synthesis of magnetic iron NPs in electrospun NFs using both conventional needle and free-surface electrospinning techniques. To the authors' knowledge such high throughput has not been previously described for NFs containing MNPs. SEM, STEM, EDX, DLS, FAAS, XRD and NMR characterization techniques indicate the presence of magnetic iron oxide NPs (magnetite) contained within polymeric NFs of a comparable quality to those produced via existing techniques. This work represents a significant step forward for production rates of magnetic NF scaffolds, in terms of both particle and fibre. This increased throughput makes the co-precipitation/electrospinning technique a viable production method for the quantities of nanofibrous scaffolds required for applications such as *in vitro* and in *vivo* tissue engineering. Different immobilisation achieved by the in-situ fabrication of the iron oxide may impact on the mechanical properties of the fibres compared to the post functionalisation procedure, this requires a comprehensive investigation in future studies. Furthermore, a suitable technique has been presented using UV irradiation for crosslinking PEO scaffolds containing MNPs to

make them suitable for applications when dissolution is not required such as in wound dressings and filter membranes.

Acknowledgements
This project is funded by the Engineering and Physical Sciences Research Council (EPSRC) and The Knowledge Economy Skills Scholarship (KESS) Project, which has been made possible by the European Union.

References

[1] T. Gong, W. Li, H. Chen, L. Wang, S. Shao, S. Zhou, Remotely actuated shape memory effect of electrospun composite nanofibres, Acta Biomater. 8 (2012) 1248–1259. doi:10.1016/j.actbio.2011.12.006.

[2] L. Qiao, X. Wang, X. Sun, X. Li, Y. Zheng, D. He, Single electrospun porous NiO-ZnO hybrid nanofibres as anode materials for advanced lithium-ion batteries., Nanoscale. 5 (2013) 3037–42. doi:10.1039/c3nr34103h.

[3] N. Nanoparticle, K. Dincer, B. Waisi, M.O. Ozdemir, U. Pasaogullari, J. Mccutcheon, Experimental Investigation of Proton Exchange Membrane Fuel Cells Operated with Nanofibre and, 9 (2015) 1406–1410.

[4] S. Ifuku, Y. Tsukiyama, T. Yukawa, M. Egusa, H. Kaminaka, H. Izawa, M. Morimoto, H. Saimoto, Facile preparation of silver nanoparticles immobilized on chitin nanofibre surfaces to endow antifungal activities, Carbohydr. Polym. 117 (2015) 813–817. doi:10.1016/j.carbpol.2014.10.042.

[5] X. Fang, H. Ma, S. Xiao, M. Shen, R. Guo, X. Cao, X. Shi, Facile immobilization of gold nanoparticles into electrospun polyethyleneimine/polyvinyl alcohol nanofibres for catalytic applications, J. Mater. Chem. 21 (2011) 4493. doi:10.1039/c0jm03987j.

[6] Z. Xu, S. Mahalingam, J.L. Rohn, G. Ren, M. Edirisinghe, Physio-chemical and antibacterial characteristics of pressure spun nylon nanofibres embedded with

functional silver nanoparticles, Mater. Sci. Eng. C. 56 (2015) 195–204. doi:10.1016/j.msec.2015.06.003.

[7] N. Cai, C. Li, C. Han, X. Luo, L. Shen, Y. Xue, F. Yu, Tailoring mechanical and antibacterial properties of chitosan/gelatin nanofibre membranes with Fe3O4 nanoparticles for potential wound dressing application, Appl. Surf. Sci. 369 (2016) 492–500. doi:10.1016/j.apsusc.2016.02.053.

[8] S.C. McBain, H.H. Yiu, J. Dobson, Magnetic nanoparticles for gene and drug delivery, Int J Nanomedicine. 3 (2008) 169–180.

[9] M. Wang, H. Singh, T.A. Hatton, G.C. Rutledge, Field-responsive superparamagnetic composite nanofibres by electrospinning, Polymer (Guildf). 45 (2004) 5505–5514. doi:http://dx.doi.org/10.1016/j.polymer.2004.06.013.

[10] T. Song, Y. Zhang, T. Zhou, C.T. Lim, S. Ramakrishna, B. Liu, Encapsulation of self-assembled FePt magnetic nanoparticles in PCL nanofibres by coaxial electrospinning, Chem. Phys. Lett. 415 (2005) 317–322. doi:http://dx.doi.org/10.1016/j.cplett.2005.09.035.

[11] P. Rujitanaroj, N. Pimpha, P. Supaphol, Wound-dressing materials with antibacterial activity from electrospun gelatin fibre mats containing silver nanoparticles, Polymer (Guildf). 49 (2008) 4723–4732.

[12] C.D. Saquing, J.L. Manasco, S.A. Khan, Electrospun Nanoparticle–Nanofibre Composites via a One-Step Synthesis, Small. 5 (2009) 944–951. doi:10.1002/smll.200801273.

[13] D.J. Thorek, A. Chen, J. Czupryna, A. Tsourkas, Superparamagnetic Iron Oxide Nanoparticle Probes for Molecular Imaging, Ann. Biomed. Eng. 34 (2006) 23–38. doi:10.1007/s10439-005-9002-7.

[14] T. Neuberger, B. Schöpf, H. Hofmann, M. Hofmann, B. von Rechenberg,

Superparamagnetic nanoparticles for biomedical applications: Possibilities and limitations of a new drug delivery system, J. Magn. Magn. Mater. 293 (2005) 483–496. doi:10.1016/j.jmmm.2005.01.064.

[15] J. Dobson, Magnetic nanoparticles for drug delivery, Drug Dev. Res. 67 (2006) 55–60. doi:10.1002/ddr.20067.

[16] A. Ito, M. Shinkai, H. Honda, T. Kobayashi, Medical application of functionalized magnetic nanoparticles, J. Biosci. Bioeng. 100 (2005) 1–11. doi:10.1263/jbb.100.1.

[17] L. Lihua, A.D. Yuris, Analysis of the effects of the residual charge and gap size on electrospun nanofibre alignment in a gap method, Nanotechnology. 19 (2008) 355307. http://stacks.iop.org/0957-4484/19/i=35/a=355307.

[18] W. Yantasee, C.L. Warner, T. Sangvanich, R.S. Addleman, T.G. Carter, R.J. Wiacek, G.E. Fryxell, C. Timchalk, M.G. Warner, Removal of heavy metals from aqueous systems with thiol functionalized superparamagnetic nanoparticles., Environ. Sci. Technol. 41 (2007) 5114–5119. doi:Doi 10.1021/Es0705238.

[19] M. Fang, P.S. Grant, M.J. McShane, G.B. Sukhorukov, V.O. Golub, Y.M. Lvov, Magnetic bio/nanoreactor with multilayer shells of glucose oxidase and inorganic nanoparticles, Langmuir. 18 (2002) 6338–6344. doi:10.1021/la025731m.

[20] H. Wei, E. Wang, Fe3O4 magnetic nanoparticles as peroxidase mimetics and their applications in H2O2 and glucose detection, Anal. Chem. 80 (2008) 2250–2254. doi:10.1021/ac702203f.

[21] M. Lewin, N. Carlesso, C.-H. Tung, X.-W. Tang, D. Cory, D.T. Scadden, R. Weissleder, Tat peptide-derivatized magnetic nanoparticles allow in vivo tracking and recovery of progenitor cells, Nat. Biotechnol. 18 (2000) 410–414.

[22] R.A. Ismail, G.M. Sulaiman, S.A. Abdulrahman, T.R. Marzoog, Antibacterial activity of magnetic iron oxide nanoparticles synthesized by laser ablation in liquid, Mater. Sci.

Eng. C. 53 (2015) 286–297. doi:http://dx.doi.org/10.1016/j.msec.2015.04.047.

[23] J. Meng, B. Xiao, Y. Zhang, J. Liu, H. Xue, J. Lei, H. Kong, Y. Huang, Z. Jin, N. Gu, H. Xu, Super-paramagnetic responsive nanofibrous scaffolds under static magnetic field enhance osteogenesis for bone repair in vivo, Sci. Rep. 3 (2013). doi:10.1038/srep02655 http://www.nature.com/srep/2013/130913/srep02655/abs/srep02655.html#supplementary-information.

[24] S. Laurent, D. Forge, M. Port, A. Roch, C. Robic, L. Vander Elst, R.N. Muller, Magnetic iron oxide nanoparticles: synthesis, stabilization, vectorization, physicochemical characterizations, and biological applications, Chem. Rev. 108 (2008) 2064–2110.

[25] J. Yeon, Y.J. Lee, D.E. Yoo, K.J. Yoo, J.S. Kim, J. Lee, J.O. Lee, S.J. Choi, G.W. Yoon, D.W. Lee, G.S. Lee, H.C. Hwang, J.B. Yoon, High throughput ultralong (20 cm) nanowire fabrication using a wafer-scale nanograting template, Nano Lett. 13 (2013) 3978–3984. doi:10.1021/nl400209n.

[26] N.M. Thoppey, J.R. Bochinski, L.I. Clarke, R.E. Gorga, Unconfined fluid electrospun into high quality nanofibres from a plate edge, Polymer (Guildf). 51 (2010) 4928–4936. doi:10.1016/j.polymer.2010.07.046.

[27] N.M. Loening, M.J. Thrippleton, J. Keeler, R.G. Griffin, Single-scan longitudinal relaxation measurements in high-resolution NMR spectroscopy, J Magn Reson. 164 (2003) 321–328.

[28] S. Meiboom, D. Gill, Modified spin- echo method for measuring nuclear relaxation times, Rev. Sci. Instrum. 29 (2004) 688–691.

[29] C. Zhou, Q. Wang, Q. Wu, UV-initiated crosslinking of electrospun poly(ethylene oxide) nanofibres with pentaerythritol triacrylate: Effect of irradiation time and

incorporated cellulose nanocrystals, Carbohydr. Polym. 87 (2012) 1779–1786. doi:10.1016/j.carbpol.2011.09.095.

[30] S.H. Tan, R. Inai, M. Kotaki, S. Ramakrishna, Systematic parameter study for ultra-fine fibre fabrication via electrospinning process, Polymer (Guildf). 46 (2005) 6128–6134. doi:http://dx.doi.org/10.1016/j.polymer.2005.05.068.

[31] O.O. Dosunmu, G.G. Chase, W. Kataphinan, D.H. Reneker, Electrospinning of polymer nanofibres from multiple jets on a porous tubular surface, Nanotechnology. 17 (2006) 1123–1127. doi:10.1088/0957-4484/17/4/046.

[32] W. Wu, Z. Wu, T. Yu, C. Jiang, W.-S. Kim, Recent progress on magnetic iron oxide nanoparticles: synthesis, surface functional strategies and biomedical applications, Sci. Technol. Adv. Mater. 16 (2015) 023501. doi:10.1088/1468-6996/16/2/023501.

[33] S. King, K. Hyunh, R. Tannenbaum, Kinetics of Nucleation, Growth, and Stabilization of Cobalt Oxide Nanoclusters, J. Phys. Chem. B. 107 (2003) 12097–12104. doi:10.1021/jp0355004.

[34] H.-Y. Lee, S.-H. Lee, C. Xu, J. Xie, J.-H. Lee, B. Wu, A.L. Koh, X. Wang, R. Sinclair, S.X. Wang, Synthesis and characterization of PVP-coated large core iron oxide nanoparticles as an MRI contrast agent, Nanotechnology. 19 (2008) 165101.

[35] Y. Gossuin, P. Gillis, a Hocq, Q.L. Vuong, a Roch, Magnetic resonance relaxation properties of superparamagnetic particles, Wiley Interdiscip. Rev. Nanobiotechnology. 1 (2009) 299–310. doi:10.1002/wnan.036.

Graphical abstract

Table of contents entry: We present a novel facile, one-step process for the in-situ synthesis of magnetic iron oxide nanoparticle-nanofibre composites using both needle and free-surface electrospinning. This is a significant step forward for production rates of magnetic nanoparticle-nanofibre scaffolds both in terms of fibre and nanoparticle production.

Keyword: Electrospinning

Luke Burke, Chris J. Mortimer, Daniel J. Curtis, Rhodri Williams, Karl Hawkins, Chris J. Wright

In-situ synthesis of magnetic iron-oxide nanoparticle-nanofibre composites using electrospinning

ToC figure